Fachtagung “Experimentelle Strömungsmechanik”
3. - 5. September 2024, Berlin

Simultaneous experimental analysis of concentration and velocity fields in gravity-driven liquid film flows over inclined smooth and microstructured surfaces

Johann Weigelt[a,b], Georg Brösigke[a], Jens-Uwe Repke[a]

[a] *Technical University of Berlin, Process Dynamics and Operations Group, Str. des 17 Juni 135, Berlin, 10623, Germany*
[b] *Corresponding author j.weigelt@tu-berlin.de*

Abstract

The study of mass transfer in multiphase mixtures is crucial for various industrial applications, requiring comprehensive consideration of numerous influencing parameters and properties. This research replicates and analyzes significant industrial phenomena on a laboratory scale using a non-invasive optical measurement system to investigate concentration and velocity fields in gravity-driven liquid film flows over inclined and microstructured surfaces. Velocity fields were measured using Particle Image Velocimetry (PIV) and concentration fields were captured through laser-induced fluorescence (LIF) with gas-sensitive dyes, resazurin and a ruthenium complex. Tests involved a glycerol-water mixture with oxygen as the gas phase. The findings indicate that surface microstructures significantly affect flow dynamics and mass transfer rates. Understanding these interactions provides valuable insights for designing and optimizing packed columns in the chemical industry. This research advances experimental fluid mechanics in multiphase flows and mass transport, highlighting the importance of surface structure in optimizing industrial processes.

Keywords: Fluid mechanics in liquid film flow, flow-structure coupling, particle image velocimetry, laser-induced fluorescence, mass transport, multiphase flow, laminar liquid flow

---

1. Introduction

Efficient control of fluid flows is crucial in chemical engineering for optimizing processes, increasing yields, and minimizing resource consumption. Gravity-driven liquid film flows are essential in industrial applications, such as packed columns used in distillation and absorption processes. The characteristics of these flows, including velocity and concentration distribution, significantly influence column performance. Understanding absorption behavior in these flows is vital for improving design and operation. Traditional invasive techniques for studying liquid film flow, like probes, can distort the flow field and limit measurement accuracy. Non-invasive optical methods, such as laser-induced fluorescence (LIF) and particle image velocimetry (PIV), provide powerful alternatives for studying thin liquid film flows without direct interaction. This study uses non-invasive optical techniques to investigate absorption behavior in gravity-driven inclined liquid film flows. It examines the impact of different surface conditions, including smooth and microstructured surfaces, on velocity profiles and concentration distributions. By analyzing the interaction between surface shape and flow behavior, the research aims to improve the design and optimization of packed columns in the chemical industry. Plates with structured surfaces and overflow weirs replicate these packing elements on a laboratory scale, focusing on the influence of microstructures on absorption behavior.

1.1. Filmflow

Liquid film flows have a relatively thin film height. The most common and studied film flow is a vertical liquid flowing down a tube or plate. Nusselt (1916) and Brauer (1956) studied film flows in the 20th century. Figure 1 shows a laminar gravity-driven film flow over an inclined smooth plate.

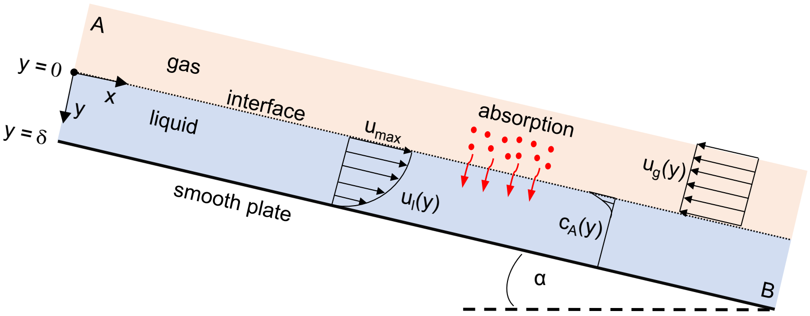

Figure 1: Two phase model of a gravity driven liquid film flow along an inclined smooth plate. Gas flow above the liquid film flow in countercurrent direction. Showing the schematic absorption process of gas molecules into the film flow.

The velocity profile $u(y)$ of a laminar film flow in Figure 1 can be described by Equation 1

$$u(y) = \frac{gsin(\alpha)\delta^2}{2\nu_f}\left(1 - \left(\frac{y}{\delta}\right)^2\right) \tag{1}$$

with y the film distance coordinate, g the gravitational acceleration, α the inclination angle of the plate, δ the film height and ν_f the kinematic viscosity of the liquid. The liquid film height δ for y = 0 can be described by Equation 2.

$$\delta = \left(\frac{3\nu_f^2}{gsin(\alpha)}\right)^{\frac{1}{3}} Re^{\frac{1}{3}} \tag{2}$$

The Reynolds number can be used to evaluate whether the liquid film flow is in a laminar, transitional, or turbulent state. Ishigai et al. (1972) has studied the Reynolds number for a liquid film flow.

$$Re = \frac{\dot{m}_l / B}{\eta_l} \tag{3}$$

with $\dot{m}_l$ the liquid mass flow, B the film flow width and η_l the dynamic viscosity of the liquid film flow.

Mass transport in the chemical industry is a critical phenomenon, but it is complex to investigate. To describe the process of mass transport analytically, the diffusion coefficient is often required, which provides essential insight into the behavior and efficiency of mass transfer. Assuming that the diffusion in flow direction and the convection flow in the y-direction can be neglected, the following partial differential equation can be obtained from Fick's law to describe the mass transport in the film flow.

$$u(y)\frac{\partial c}{\partial x} = -D\frac{\partial^2 c}{\partial y^2} \tag{4}$$

Analytical solutions already exist to solve the partial differential equation for certain assumptions. Near the interface the analytical solution is a complementary error function, shown in Equation 5. A more detailed derivation was made by Bird et al. (2002).

$$\frac{c_A(y)}{c_0} = 1 - \mathrm{erf}\left(\frac{y}{\sqrt{4D/u_{max}}}\right) = 1 - \mathrm{erf}\left(\frac{y}{2\sqrt{Dt}}\right) \tag{5}$$

The effect of a chemical reaction on the mass transfer is that the concentration gradient of the diffusing component increases as a result of the degradation reaction, thereby intensifying the mass transfer. This chemical reaction effect can be measured by using the enhancement factor.

$$E = \frac{\beta_{l,R}}{\beta_{l,nR}} \tag{6}$$

where $\beta_{l,R}$ is the local mass transfer coefficient with reaction and $\beta_{l,nR}$ is without reaction.

1.2. Coupling structure and flow

Modern high performance packings in packed columns in the chemical industry have microstructures as well as macrostructures. These are thought to influence both surface wetting and liquid mixing Kohrt (2012). Simplified geometries have been analysed to be able to identify general relationships by using model systems (Davies (1972), Zhao and Cerro (1992)). Figure 2 shows a smooth plate and a plate with a 2 dimensional step structure.

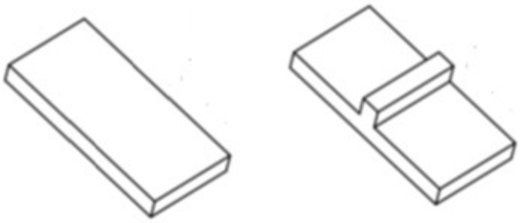

Figure 2: Smooth plate (left) and plate with a 2 dimensional step structure (right)

The experiments of Zhao and Cerro (1992) were carried out on two-dimensional structured plates at small Re numbers up to $Re = 9.1$ by varying the film height and the flow rate of different solvents (glycerol $\eta = 450$ to 938 mPa s, pure water and glycerol-water mixtures $\eta =$

6.8 to 19.5 mPa s. They developed the dimensionless ratio δ^*, which describes the relationship between Nusselt film height and structure height. They found that this ratio gives important insights on the influence of the structure on the flow. This should be taken into account when designing the structures.

$$\delta^* = \frac{\delta_N}{A} \tag{7}$$

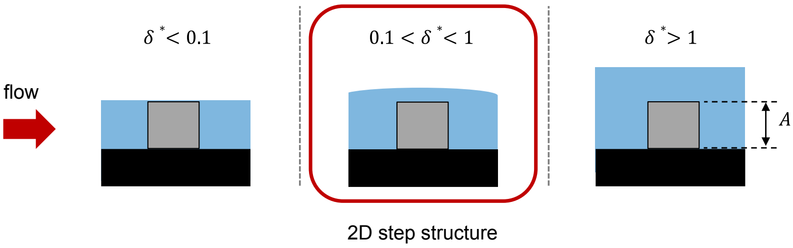

Figure 3: Influence of the ratio between Nusselt film height and 2 dimensional structure height δ^* on the liquid film flow.

$\delta^* < 0.1$	The film flow follows the surface structure and approximates the shape of a quasi-fully-developed flow on inclined plates.
$0.1 < \delta^* < 1$	In this range we have a stronger influence of the surface structure onto the liquid film flow. For industrially interesting flow rates, flow control in the medium to high range ($\delta^* \approx 1$) is recommended for microstructures.
$\delta^* > 1$	The film flow has an almost smooth surface, similar to a smooth plate. The surface structure has no influence on the liquid film flow.

1.3. Optical measurement techniques

In the chemical industry, laser-induced fluorescence (LIF) is primarily used for the analysis of trace components in complex mixtures. Its high sensitivity allows the detection of minute concentrations of analytes, which is critical for quality control and process monitoring. LIF is based on the excitation of the dye molecules by a laser beam, which raises the dye molecules to an excited, higher energy state. Upon returning to the ground state, these molecules emit characteristic fluorescent light that can be captured by cameras. Analysis of the captured intensities provides insight into the local concentration.

Particle Image Velocimetry (PIV) is a validated experimental technique widely used in various fields for flow visualization and quantitative analysis. PIV works by seeding the fluid of interest with tracer particles and illuminating the particles with a laser beam. A camera captures consecutive images of the illuminated particles, and cross-correlation algorithms process these images to determine the displacement of the particles between frames, thus providing velocity fields.

Based on the literature on liquid mass transport and non-invasive optical measurement methods, the study aims to simultaneously measure velocity and concentration profiles in film flows over different surface geometries on a laboratory scale in order to gain fundamental knowledge of these physical processes.

2. Materials and methods

2.1. Experimental setup

The experimental configuration, shown in Figure 4, revolved around a photoluminescence imaging system in combination with a particle image velocemitry system, specifically designed for the investigation for a liquid-gas multiphase LIF and PIV configurations. These measurement methods were selected because they enable the non-invasive and accurate optical measurement of the velocity and concentration fields required for identifying the mass transport. We used 100 mg L^{-1} resazurin or 20 mg L^{-1} of rutheniumcomplex as oxygen sensitive dyes for LIF. The seeding particles for PIV had a diameter of 10 µm (HGS, Dantec Dynamics).

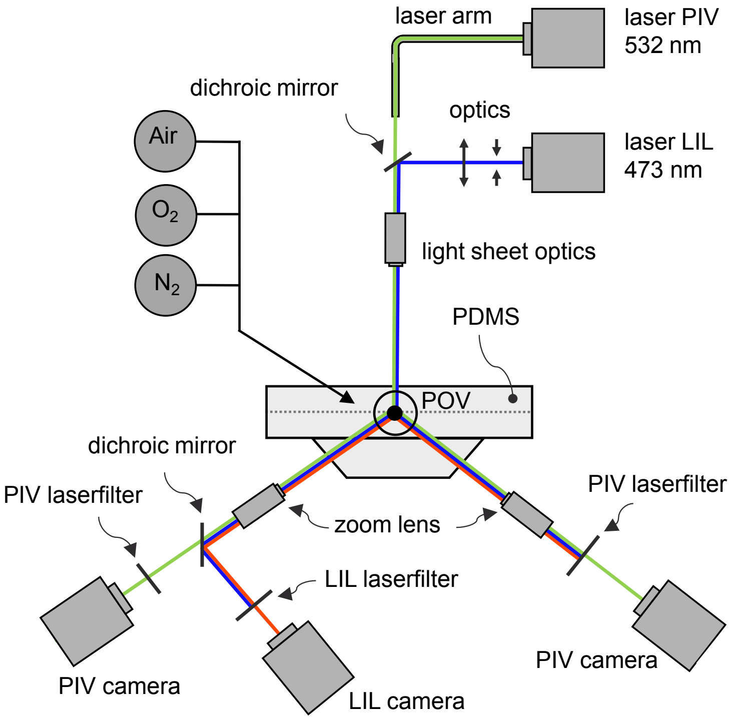

Figure 4: Experimental setup: coupled PLIF, PLIF-I and stereo PIV setup with laser in front of target and camera system behind. Mass flow controller for gas flow [mod. Gerke et al. (2024)]

The 16 bit 5.5 Megapixel sCMOS camera (Hisense Zyla 5.5 USB3, Andor) captured the fluorescence signal at a frame rate of 10 Hz in combination with a magnification system by Navitar 4k zoom with 0.5x lens attachment and a 570 nm high-pass filter (Dantec Dynamics). The oxygen-sensitive dyes were excited with a 50 mW continuous wavelength laser (MBL-III-473-50-3-LED, CNI) and the gas phase was adjusted with a mass flow controller (EL-FLOW Select F-201CV, Bronkhorst). The examined liquid comprised deionized water and a glycerol-based (CAS 56-81-5). We used a mixture of 58.5 to 41.5 wt.% glycerol and water, which was applied as a film flow through an overflow weir onto custom made PDMS plates.

2.2. Dyes

The oxygen sensitive dyes investigated in the study are a ruthenium complex (Tris-(4.7-diphenyl-1.10-phenanthrolin)-ruthenium chloride, CAS 36309-88-3) and resazurin (7-hydroxy-3h-phenoxazin-3-on-10-oxid, CAS 62758-13-8). The dyes work on different principles. The fluorescent light emitted by the ruthenium complex is reduced by oxygen molecules according to the Stern-Vollmer equation. Resazurin, on the other hand, requires the presence of oxygen to become fluorescent under laser light. Resazurin must be reduced to dihydroresorufin for experiments. The dihydroresorufin then reacts with oxygen and forms resorufin, which is fluorescent. The reaction scheme for resazurin is visualized in Figure 5.

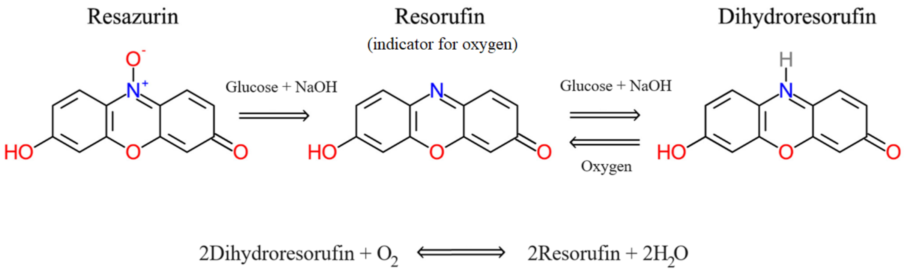

Figure 5: Scheme for pseudoreversible reaction between resorufin and dihydroresorufin involving, glucose, sodium hydroxid and oxygen. Dihydroresorufin is colorless, while the oxygen indicator resorufin is reddish. [mod. Knapp et al. (2018)]

3. Results

In this section, we present the preliminary results of our study. These will be further expanded and discussed as the conference take place. The LIF image presented in Figure 6 and Figure 7 depicts the intensity fields for both a smooth plate and a plate with a step-structure surface. High-intensity regions indicate elevated oxygen concentrations. The images confirm that the liquid-gas interface remains uncurved for the smooth plate, unlike the step-structured plate. This detailed visualization is crucial for analyzing fluid flow behavior across different geometries, shedding light on phenomena such as recirculation zones and enhanced mixing. Notably, the observed intensity at the bottom of the image suggests potential oxygen transport through the film flow or oxygen release from the PDMS material, necessitating further investigation. A detailed examination of the intensity image of the smooth plate allows for the determination of intensity or concentration profiles for each x position. Figure 6 illustrates the raw image and the corresponding normalized concentration profile at the middle x position of the film flow. Similarly, Figure 7 applies this approach to the plate with a step structure, offering a comparative analysis of concentration profiles between different geometries. Both figures demonstrates that the normalized concentration profile, as determined by experimental measurements, exhibits a qualitative resemblance to a complementary error function.

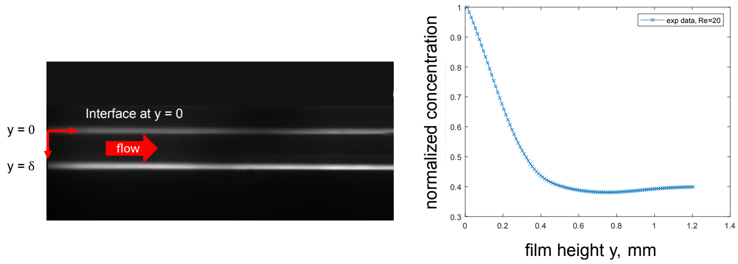

Figure 6: Raw intensity image of a smooth plate for the tracer dye resazurin (left side) normalized concentration profile for the middle location of the filmflow (right side). Re = 30, α = 10°, T = 293.15K

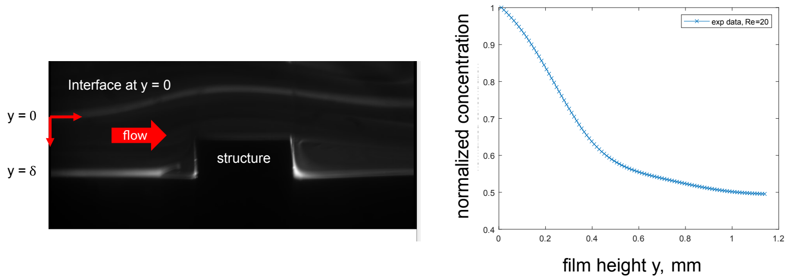

Figure 7: Raw intensity image of a step structure for the tracer dye resazurin (left side) normalized concentration profile for the middle location of the filmflow (right side). Re = 30, α = 10°, T = 293.15K

Figure 8 presents the flow analysis for the smooth plate. The top left panel displays the raw image of seeding particles. The bottom left panel shows the normalized flow field with individual velocity profiles plotted over the film height. The right panel compares the analytical and experimental velocity fields (Re = 80, α = 10°, T = 293.15K), demonstrating good agreement between them. The film thickness is measured to be approximately 1 mm.

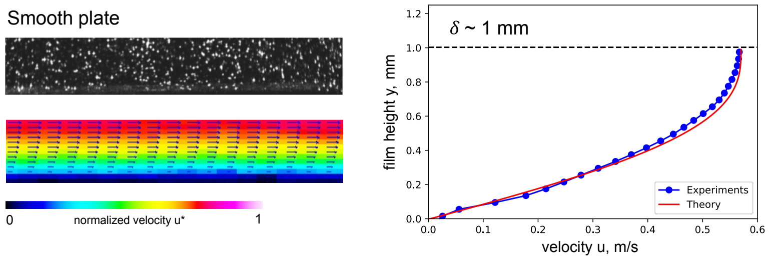

Figure 8: Raw particle image and normalized velocity profiles of a smooth plate with PIV (left side). Comparison of the experimental and theoretical velocity profiles (right side). Re = 80, α = 60°, T = 293.15K

Figure 9 compares the flow analyses of the smooth plate and the plate with a step structure. The top left panel presents the normalized flow field for the smooth plate, while the bottom left panel displays the flow field for the plate with a step structure. The right panel features the velocity field from both the analytical solution and experimental values for the smooth plate. Velocity profiles at three different positions within the film flow are also plotted, showing identical profiles before and after the structure but significant transformation during the structure. Notably, there is a reduction in film flow velocity u just before the structure at position 2. This is attributed to the flow being redirected around the structure.

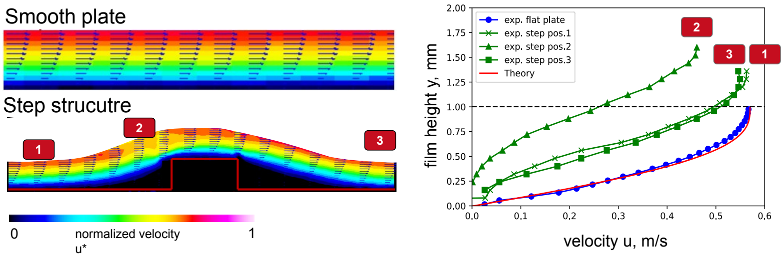

Figure 9: Normalized velocity profiles of a smooth plate and step structure plate with PIV (left side). Comparison of the experimental velocity profiles for different local positions in the film flow (right side). Re = 80, α = 60°, T = 293.15K

4. Conclusion

The study demonstrates the feasibility of using a non-invasive optical measurement system to simultaneously analyze concentration and velocity fields in gravity-driven liquid film flows over inclined, microstructured surfaces. Using Particle Image Velocimetry (PIV) and Laser Induced Fluorescence (LIF) with gas sensitive dyes, we achieved detailed visualizations and quantitative assessments of flow dynamics and mass transfer processes on a laboratory scale. The experimental results indicate an influence of surface microstructures on the flow, in particular showing different film flow velocities in the vicinity of structural features. These results confirm the effectiveness of the system for detailed fluid flow analysis and provide valuable insights for optimizing industrial applications involving multiphase mixtures and complex surface geometries. This approach promises accurate representations of near-industrial conditions.

5. Acknowledgement

Gefördert durch die Deutsche Forschungsgemeinschaft (DFG) - 466839600 / funded by the Deutsche Forschungsgemeinschaft (DFG, German Research Foundation) – 466839600.

References

Bird, R.B., Stewart, W.E., Lightfoot, E.N., 2002. Transport phenomena. 2nd ed., Wiley, New York. ISBN: 0-471-41077-2.

Brauer, H., 1956. Strömung und Wärmeübergang bei Rieselfilmen. Bericht / Max-Planck-Institut für Strömungsforschung, VDI, Düsseldorf 457.

Davies, J.T., 1972. Turbulence phenomena at free surfaces. AIChE Journal 18, 169–173. doi:10.1002/aic.690180131.

Gerke, S.J., Brösigke, G., Repke, J.U., 2024. Planar light induced fluorescence quenching oxygen diffusivity measurement near the gas–liquid interface in aqueous glycerol and aqueous propylene glycol. Experimental Thermal and Fluid Science 153, 111131. doi:10.1016/j.expthermflusci.2023.111131.

Ishigai, S., Nakanisi, S., Koizumi, T., Oyabu, Z., 1972. Hydrodynamics and heat transfer of vertical falling liquid films : Part 1, classification of flow regimes. Bulletin of the JSME 15, 594–602. doi:10.1299/jsme1958.15.594.

Knapp, J.L.A., González-Pinzón, R., Haggerty, R., 2018. The resazurin–resorufin system: Insights from a decade of "smart" tracer development for hydrologic applications. Water Resources Research 54, 6877–6889. doi:10.1029/2018WR023103.

Kohrt, M., 2012. Experimentelle untersuchung von stofftransport und fluiddynamik bei rieselfilmströmungen auf mikrostrukturierten oberflächen. doi:10.14279/depositonce-3208.

Nusselt, W., 1916. Die Oberflächenkondensation des Wasserdampfes. VDI, Frankfurt, 60, 541-546, 569-575.

Zhao, L., Cerro, R.L., 1992. Experimental characterization of viscous film flows over complex surfaces. International Journal of Multiphase Flow 18, 495–516. doi:10.1016/0301-9322(92)90048-L.